Am J Transl Res 2026;18(5):3926-3941
www.ajtr.org /ISSN:1943-8141/AJTR0168989

Original Article

Salvianolic acid B protects cardiac function via β3-AR/miRNA-1 axis-mediated cardiomyocyte proliferation in myocardial infarction rats

Biao Li, Fang Zeng, Haoyang Ge, Qiang Zhao

Department of Cardiology, Guangzhou Red Cross Hospital of Jinan University, Guangzhou 510220, Guangdong, China

Received September 24, 2025; Accepted April 8, 2026; Epub May 15, 2026; Published May 30, 2026

Abstract: Objective: To investigate whether Salvianolic Acid B (SAB) promotes cardiomyocyte proliferation by activating the β3-adrenergic receptor (β3-AR)/microRNA-1 (miR-1) axis, thereby improving cardiac function following myocardial infarction. Methods: A rat model of myocardial infarction was established using left anterior descending artery ligation. Rats were randomly divided into 7 groups: sham surgery group, MI group, MI + SAB group, MI + β3-AR agonist group, MI + SAB + β3-AR antagonist group, MI + SAB + miR-1 mimic group, and MI + negative control RNA group. Echocardiography was used to assess cardiac function; TTC, Masson's, and H&E staining were used to evaluate infarct, fibrosis, and necrosis areas; and Ki67 immunohistochemistry was used to detect cardiomyocyte proliferation. In vitro experiments utilized a hypoxia/reoxygenation (H/R) model in neonatal rat cardiomyocytes, with interventions including SAB, β3-AR modulators, or miR-1 mimics/inhibitors. Cell proliferation was assessed using EdU staining, while molecular mechanisms were examined via qPCR, Western blot, and dual-luciferase reporter assays. Results: SAB treatment significantly improved left ventricular ejection fraction (LVEF) and fractional shortening (LVFS) in MI rats, reduced infarct and fibrosis areas, and increased the proportion of Ki67-positive cardiomyocytes. Mechanistically, SAB upregulated β3-AR expression, downregulated miR-1 expression, and increased the protein levels of miR-1 target genes CDK4 and Cyclin D1. β3-AR antagonists or miR-1 mimic could block the aforementioned protective effects of SAB. In vitro experiments confirmed that SAB promoted EdU incorporation in H/R-injured cardiomyocytes, downregulated miR-1, and upregulated Cyclin D1; β3-AR antagonist or miR-1 mimic could eliminate these effects. Dual luciferase reporter assays confirmed that miR-1 directly targets the 3'UTR of CDK4. Conclusion: SAB improves cardiac function after myocardial infarction by activating the β3-AR/miR-1 axis, thereby lifting miR-1's inhibition of CDK4 and Cyclin D1 and promoting cardiomyocyte proliferation. This study reveals a novel mechanism underlying the cardioprotective effects of SAB and identifies the β3-AR/miR-1 axis as a potential therapeutic target for cardiac regeneration following myocardial infarction.

Keywords: Salvianolic acid B, β3-adrenergic receptor, microRNA-1, myocardial infarction, cardiomyocyte proliferation, cardiac remodeling

Introduction

Myocardial infarction (MI) remains one of the leading causes of heart failure, primarily due to the extremely limited endogenous regenerative capacity of adult cardiomyocytes [1, 2]. Following myocardial infarction, a large number of cardiomyocytes undergo necrosis and apoptosis, and adult cardiomyocytes struggle to replace the lost functional myocardial tissue through proliferation. This triggers a series of pathological cascades, ultimately leading to myocardial fibrosis, ventricular remodeling, and progressive decline in cardiac function [3, 4]. Although reperfusion therapies (such as percutaneous coronary intervention) have significantly reduced mortality in the acute phase of myocardial infarction, their primary role is to salvage myocardial tissue in the ischemic border zone; they cannot effectively promote myocardial tissue regeneration and functional recovery [5-7]. Therefore, exploring new strategies capable of activating adult cardiomyocyte proliferation, inhibiting pathological remodeling, and promoting functional cardiac repair has become a critical scientific issue and an important frontier in

https://doi.org/10.62347/IXXD9674

cardiovascular research that urgently needs to be addressed [8, 9].

Salvianolic Acid B (SAB) is one of the most abundant water-soluble bioactive components in the traditional Chinese medicinal herb Salvia miltiorrhiza and has been demonstrated to exert multi-targeted cardioprotective effects in various cardiovascular disease models [10, 11]. Existing studies indicate that SAB can significantly alleviate oxidative stress damage, suppress inflammatory responses, reduce cardiomyocyte apoptosis, and improve microcirculatory function [12-14]. These findings provide preliminary experimental evidence for the potential application of SAB in cardiac repair following myocardial infarction. However, little is currently known regarding whether SAB can directly stimulate cardiomyocytes to enter the cell cycle and proliferate, or about the precise molecular regulatory network underlying its promotion of cardiac function recovery - particularly the mechanisms involving key signaling pathways and downstream effector molecules - and these aspects require further elucidation [15, 16].

The β3-adrenergic receptor (β3-AR) is classically recognized as being primarily expressed in adipose tissue, where it mediates catecholamine-induced lipolysis and thermogenesis, playing a key role in the regulation of energy metabolism [17]. In recent years, a growing body of evidence has revealed the “non-classical” expression and function of β3-AR in the cardiovascular system. Although its expression levels in cardiac muscle are far lower than those of the dominant β1-AR and β2-AR subtypes, activation of β3-AR exhibits unique cardioprotective effects [18]. In models of myocardial ischemia/reperfusion injury, heart failure, and cardiomyopathy, β3-AR activation has been shown to exert cardioprotective effects through multiple mechanisms: including activation of the endothelial nitric oxide synthase (eNOS) pathway to enhance the bioavailability of nitric oxide (NO), thereby exerting anti-apoptotic effects; improving the energy metabolism efficiency of cardiomyocytes by optimizing the utilization of fatty acids and glucose; and downregulating the excessive activation of the renin-angiotensin-aldosterone system (RAAS), thereby mitigating its adverse effects of promoting fibrosis and cardiomyopathy [19]. These findings position β3-AR as a promising target for cardioprotection. However, a critical and as yet unexplored question remains: Can β3-AR activation directly drive the proliferation of adult cardiomyocytes? [20] Specifically, within the complex microenvironment of cardiac repair following myocardial infarction, does the β3-AR signaling pathway participate in regulating the process by which cardiomyocytes exit terminal differentiation, re-enter the cell cycle, and undergo mitotic proliferation? Research in this direction holds significant potential value and innovation [21, 22].

MicroRNAs (miRNAs) are a class of non-coding small RNA molecules approximately 22 nucleotides in length that finely regulate the expression of more than 60% of mammalian genes at the post-transcriptional level, primarily by promoting the degradation of target mRNAs or inhibiting their translation [23]. In the heart, specific miRNAs have been identified as central regulatory factors governing cardiac development, maintenance of homeostasis, and pathological processes such as hypertrophy, fibrosis, and impaired regeneration [24]. Among these, miRNA-1 (miR-1) is widely recognized as a heart-enriched miRNA due to its high abundance and specific expression in cardiomyocytes. Crucially, miR-1 plays a key role in maintaining the terminally differentiated state of cardiomyocytes. It does so by simultaneously targeting and inhibiting multiple cell cycle-positive regulators (such as cyclin-dependent kinase 4 (CDK4), cyclin D1 (Cyclin D1), cyclin-dependent kinase 6 (CDK6), histone deacetylase 4 (HDAC4), and insulin-like growth factor 1 (IGF-1)), acting as a powerful molecular “brake” that prevents cardiomyocytes from re-entering the cell cycle [25]. Therefore, inhibiting the expression or activity of miR-1 after myocardial infarction could theoretically lift the inhibition on the cell cycle engine, thereby restoring the proliferative capacity of cardiomyocytes. Interestingly, G protein-coupled receptors (GPCRs) - the largest family of cell surface receptors - have been shown to profoundly influence the expression profiles of specific miRNAs through their downstream signaling pathways (e.g., cAMP/PKA, PKC, MAPK) upon activation [26]. Various plant-derived natural compounds (such as resveratrol and ginsenosides) have been reported to regulate miRNAs by activating specific GPCRs, thereby influencing cellular behavior [27]. This raises a thought-provoking scientific hypothesis: Could SAB, as a natural compound with

a complex phenolic acid structure, act as (or resemble) a GPCR ligand - possibly targeting β3-AR - and, by activating this receptor and its downstream signaling network, ultimately lead to downregulation of miR-1 expression? Such regulation might be achieved by influencing miR-1's transcription factors or epigenetic modification mechanisms.

Based on the above background, this study proposes the following scientific hypothesis: Salvianolic Acid B (SAB) downregulates miRNA-1 (miR-1) expression by activating the β3-adrenergic receptor (β3-AR), thereby lifting its inhibition of the cell cycle positive regulators CDK4 and Cyclin D1, promoting cardiomyocyte proliferation, and ultimately improving cardiac function following myocardial infarction. To test this hypothesis, we will utilize a rat myocardial infarction model and a primary cardiomyocyte hypoxia/reoxygenation (H/R) injury model to conduct the following studies: (1) Evaluate whether SAB enhances cardiomyocyte proliferation (using markers such as Ki67 and EdU), improves cardiac function (LVEF, LVFS), and reduces pathological remodeling; (2) Verify the critical role of β3-AR in mediating the effects of SAB using specific β3-AR agonists and antagonists; (3) To determine the effects of SAB and β3-AR activation on miR-1 expression in cardiomyocytes, and to establish a causal relationship between its proliferative effects using miR-1 mimic and inhibitor; (4) To confirm the upregulation of key miR-1 targets (CDK4, Cyclin D1) and associate this with cell cycle re-entry regulated by the β3-AR/miR-1 axis. By elucidating the signaling axis "SAB → β3-AR activation → miR-1 downregulation → cardiomyocyte proliferation → improved cardiac function," this study aims to reveal a novel mechanism underlying the cardioprotective effects of SAB and to establish the β3-AR/miR-1 axis as a potential therapeutic target for cardiac repair following myocardial infarction.

Materials and methods

Laboratory animals

Male SPF Sprague-Dawley rats weighing 250-280 g were purchased from the Laboratory Animal Center of our institute. Animals were housed in a controlled environment with constant temperature (22 ± 2°C), constant humidity (50 ± 5%), and a 12-hour light/dark cycle, with free access to food and water. All animal experiments were approved by the Guangzhou Red Cross Hospital of Jinan University Ethics Committee and conducted in accordance with the "Guidelines for the Care and Use of Laboratory Animals".

In vivo experiments

Establishment of the myocardial infarction model and grouping: A myocardial infarction model was established using the left anterior descending (LAD) artery ligation method. After anesthetizing rats with intraperitoneal injection of 1% sodium pentobarbital (50 mg/kg), tracheal intubation was performed and the rats were connected to a ventilator. A thoracotomy was performed at the fourth left intercostal space to expose the heart, and the LAD was ligated approximately 2 mm below the left atrial appendage using 6-0 silk suture. A successful model was defined by pallor of the left ventricular anterior wall and ST-segment elevation on the electrocardiogram following ligation. The sham group (Sham) underwent threading without ligation [6, 8].

Rats were randomly divided into 7 groups (n = 6-8/group):

(1) Sham group: Sham surgery; no intervention. (2) MI group: LAD ligation; no pharmacological intervention. (3) MI + SAB group: Following LAD ligation, intraperitoneal injection of 10 mg/kg/day of Salvianolic Acid B (SAB, purity ≥98%, Sigma-Aldrich, Cat# SML2968) for 28 consecutive days. (4) MI + β3-AR Agonist Group: Following LAD ligation, intraperitoneal injection of the β3-AR agonist BRL37344 (Cayman Chemical, Cat# 10006618) at 1 mg/kg/day for 28 consecutive days. (5) MI + SAB + β3-AR antagonist group: Following LAD ligation, SAB (10 mg/kg/day) and the β3-AR antagonist SR59230A (0.5 mg/kg/day) were administered intraperitoneally simultaneously for 28 consecutive days. (6) MI + SAB + miR-1 mimic group: Three days prior to LAD ligation, an adenoviral vector carrying the miR-1 mimic (sequence: 5'-UGGAAUGUAAAGAAGUAUGUAU-3') was administered via the tail vein (titer 1×10^9 PFU/mL, 200 μL/animal); following LAD ligation, SAB (10 mg/kg/day) was administered intraperitoneally for 28 days. (7) MI + Negative Control RNA Group: Three days prior to LAD ligation, rats received a tail vein injection of liposome-encapsulated negative control RNA (sequence: 5'-UUCUCCGAACGUGUCACGUTT-3', 50 mg/kg) as a negative control for nucleic acid intervention.

Echocardiography: Twenty-eight days post-surgery, cardiac echocardiography was performed using a Vevo 2100 ultrasound system (VisualSonics). Rats were anesthetized with 1% isoflurane via inhalation. M-mode echocardiographic images were acquired using a parasternal long-axis view of the left ventricle. Left ventricular ejection fraction (LVEF), left ventricular fractional shortening (LVFS), left ventricular end-diastolic diameter (LVEDD), and left ventricular end-systolic diameter (LVESD) were measured. The average value from three consecutive cardiac cycles was recorded for each rat.

Euthanasia and tissue collection: Following the echocardiography, rats were euthanized by intraperitoneal injection of a lethal dose of sodium pentobarbital (150 mg/kg). Criteria for confirming death included: cessation of heartbeat and respiration for more than 5 minutes, loss of corneal reflex, and onset of rigor mortis. The heart was rapidly removed, rinsed with ice-cold saline, and blood was removed. The heart was divided into three parts: one portion was used for TTC staining; another was fixed in 4% paraformaldehyde for histological analysis; and the remaining portion was immediately frozen in liquid nitrogen and transferred to a -80°C freezer for molecular biological testing.

Histological analysis: TTC staining: Heart tissue sections (approximately 2 mm thick) were placed in a 1% 2,3,5-triphenyl-tetrazolium chloride (TTC) solution and incubated at 37°C in the dark for 15 minutes. Normal myocardium appeared red, while infarcted myocardium appeared pale. The infarct area was calculated using ImageJ software (percentage of infarct area = infarct area/total left ventricular area × 100%).

Masson's trichrome staining: Paraffin-embedded ventricular tissue sections (5 μm) were deparaffinized in water and processed according to the instructions of the Masson's trichrome staining kit. Collagen fibers appear blue, and cardiomyocytes appear red. Five non-overlapping fields of view (×200) were randomly selected from each section, and the percentage of blue collagen area relative to the total tissue area was calculated using ImageJ software, representing the fibrosis area.

H&E staining: Paraffin sections (5 μm) were routinely deparaffinized and stained with hematoxylin and eosin. Pathological changes such as cardiomyocyte necrosis and inflammatory infiltration were observed. Five fields of view (×200) were randomly selected from each section and ImageJ was used to measure the percentage of necrotic area (necrotic area = area of necrotic region/total field area × 100%).

Ki67 Immunohistochemistry: Paraffin sections (5 μm) were subjected to high-pressure heat retrieval in citrate buffer, followed by blocking of endogenous peroxidase with 3% hydrogen peroxide and blocking with 10% goat serum. Rabbit anti-Ki67 primary antibody (1:200, Cell Signaling Technology, Cat# 9129) was applied °C overnight; the following day, HRP-labeled secondary antibody was added, followed by DAB staining and counterstaining with hematoxylin. Brownish-red cell nuclei were considered positive. In the peri-infarct zone of each section, 5 random high-power fields (×400) were selected, and the percentage of Ki67-positive myocardial cell nuclei relative to all myocardial cell nuclei was calculated.

In vitro experiments

Isolation and culture of neonatal rat cardiomyocytes: SD neonatal rats aged 1-2 days were used. Hearts were harvested after disinfection with 75% ethanol. Ventricular tissue was excised and digested repeatedly for 15-20 minutes at 37°C for 15-20 minutes, cell suspension was collected, filtered through a 70-μm mesh, and fibroblasts were removed using the differential adhesion method (by placing the cell suspension in an uncoated culture dish and allowing it to stand for 2 hours). The non-adherent cardiomyocytes were resuspended in DMEM medium containing 10% fetal bovine serum (FBS), 100 U/mL penicillin, and 100 μg/mL streptomycin, and seeded onto 0.1% gelatin-coated culture dishes or glass slides. They were then cultured in a 37°C, 5% CO_2 incubator. The medium was changed every 48 h.

Hypoxia/reoxygenation (H/R) model and treatment: 48 hours after cell seeding, the medium was replaced with sugar-free DMEM and cultured in a hypoxic incubator (1% O_2, 5% CO_2, 94% N_2) for 6 hours. The medium was then replaced with normal medium containing 10% FBS, and culturing was continued in a normal incubator for 18 hours, thereby establishing the H/R injury model.

The following treatment groups were established based on experimental requirements:

H/R group: H/R treatment only.

H/R + SAB group: SAB (10 μM) was added 24 hours prior to H/R treatment.

H/R + β3-AR agonist group: BRL37344 (1 μM) was added 24 hours prior to H/R treatment.

H/R + SAB + β3-AR antagonist group: SAB (10 μM) and SR59230A (0.5 μM) were added simultaneously 24 h prior to H/R treatment.

H/R + SAB + miR-1 mimic group: 24 h prior to H/R treatment, transfect with miR-1 mimic (50 nM) using Lipofectamine 3000, followed by H/R treatment with SAB.

H/R + miR-1 inhibitor group: Transfected with miR-1 inhibitor (50 nM) 24 h prior to H/R treatment, followed by H/R treatment (without SAB).

H/R + Negative Control RNA group: Transfected with negative control RNA (50 nM) 24 h prior to H/R treatment, followed by H/R treatment.

All transfections were performed according to the Lipofectamine 3000 protocol, and transfection efficiency was verified in preliminary experiments.

Assessment of cell proliferation: EdU incorporation assay: After cell treatment, EdU (50 μM) was added to the culture medium, and the cells were incubated at 37°C for 2 hours. Cells were fixed with 4% paraformaldehyde, permeabilized with 0.5% Triton X-100, stained with Apollo 567, and nuclei were counterstained with DAPI. Under a fluorescence microscope (×200), at least 500 cells per well were randomly counted and the percentage of EdU-positive cells was calculated.

CCK-8 assay: After cell treatment, 10 μL of CCK-8 solution was added to each well and incubated at 37°C for 2 h. Cell viability was determined by measuring the absorbance at 450 nm using a microplate reader.

Dual luciferase reporter assay: A luciferase reporter plasmid (pmirGLO-CDK4-3'UTR) containing the 3' untranslated region (3'UTR) of the human CDK4 gene was constructed. HEK293T cells were seeded in a 24-well plate. When confluence reached 70%, Lipofectamine 3000 was used to co-transfect the cells with pmirGLO-CDK4-3'UTR (200 ng/well), miR-1 mimetic or negative control (50 nM), and the sea-kidney luciferase internal control plasmid (20 ng/well) using Lipofectamine 3000. Forty-eight hours after transfection, cells were lysed according to the instructions of the Dual Luciferase Report Assay Kit (Promega). Firefly luciferase and sea-cuttlefish luciferase activities were measured, and the ratio of the two was calculated as the relative luciferase activity.

Molecular biology assays

Real-time quantitative PCR (qPCR): Total RNA was extracted from cardiac tissue or cardiac cells using TRIzol reagent. Reverse transcription: For mRNA, cDNA was synthesized using the PrimeScript RT Kit (TaKaRa); for miRNA, tailing reverse transcription was performed using the Mir-X miRNA First-Strand Synthesis Kit (TaKaRa).

qPCR reaction system: 10 μL SYBR Green PCR Master Mix (Applied Biosystems), 0.4 μL each of forward and reverse primers, 1 μL cDNA template, and water to a total volume of 20 μL. Reaction conditions: 30 s pre-denaturation at 95°C; denature at 95°C for 5 s, anneal at 60°C for 30 s, for a total of 40 cycles; followed by melting curve analysis. Relative expression levels were calculated using the 2-ΔΔCt method. β-actin was used as the internal control for mRNA, and U6 snRNA was used as the internal control for miRNA. Primer sequences are shown in **Table 1**.

Western blot: Tissues or cells were lysed using RIPA lysis buffer containing protease and phosphatase inhibitors. The supernatant was collected by centrifugation at 4°C, and protein concentration was determined using the BCA assay. Equal amounts of protein (30-50 μg) were separated by 10% SDS-PAGE and wet-transferred to a PVDF membrane. The membrane was blocked with 5% non-fat dry milk at room temperature for 1 h, then incubated with the following primary antibodies: rabbit anti-β3-AR (1:1000, CST, Cat# 14989); rabbit anti-Ki67 (1:1000, CST, Cat# 9129); rabbit anti-CDK4 (1:1000, CST, Cat# 12790); rabbit anti-Cyclin D1 (1:1000, CST, Cat# 55506); mouse anti-GAPDH (1:5000, CST, Cat# 5174) at 4°C overnight. After washing the membranes with TBST,

Table 1. qPCR primer sequences

Gene	Forward Primer (5' → 3')	Reverse Primer (5' → 3')
miRNA-1	CTCAACTGGTGTCGTGGAGTCGGCA	GCAGTGCAGGGTCCGAGGT
U6 (snRNA)	CTCGCTTCGGCAGCACA	AACGCTTCACGAATTTGCGT
CDK4	CCCAGCAAGATGGAGAAGGA	GCTGGATGTTCTGGGCTTGG
CCND1 (Cyclin D1)	TGGAGCCCCTGAAGAAGTTG	CAGGTCCAGGTGGGTGTGAA
β3-AR	ATGCTGCTGCTGCTGCTGTT	TCAGGTGGTGGTGGTGGTGA
β-actin	GGAGATTACTGCCCTGGCTCCTA	GACTCATCGTACTCCTGCTTGCTG

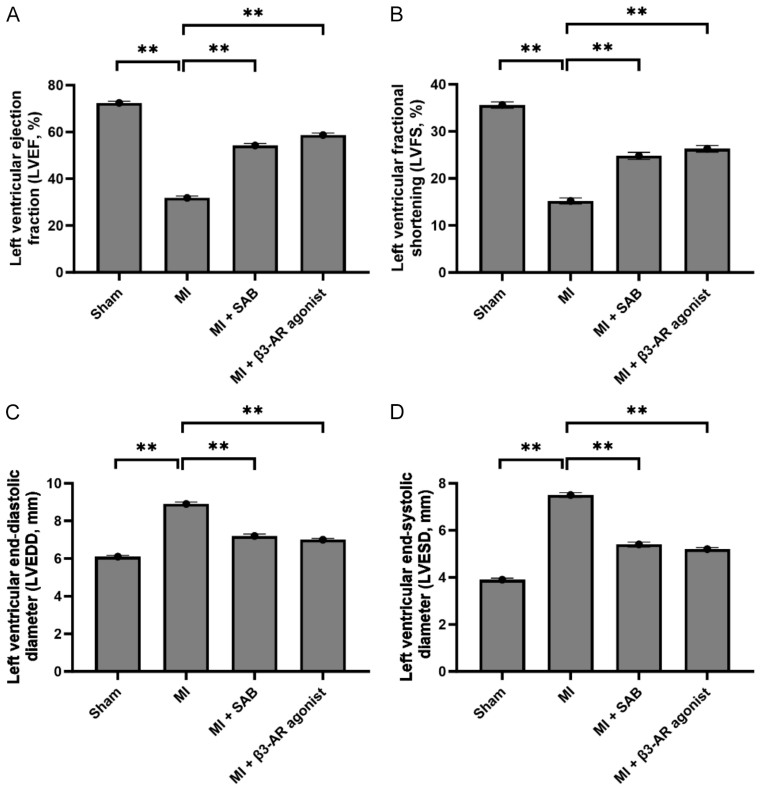

Figure 1. SAB improves cardiac function in MI rats. A: Left ventricular ejection fraction (LVEF, %). B: Left ventricular fractional shortening (LVFS, %). C: Left ventricular end-diastolic diameter (LVEDD, mm). D: Left ventricular end-systolic diameter (LVESD, mm). Data are presented as mean ± SEM (n = 8 per group). **P < 0.01 vs. MI group (one-way ANOVA with Tukey's post hoc test).

they were incubated with HRP-labeled secondary antibodies at room temperature for 1 hour, followed by ECL chemiluminescence detection. Band intensity values were analyzed using ImageJ software, and relative expression levels were expressed as the intensity ratio of the target protein to GAPDH.

Statistical analysis

All data are expressed as mean ± standard error of the mean (mean ± SEM). Comparisons among multiple groups were performed using one-way ANOVA, with Tukey's post-hoc test for pairwise comparisons; comparisons between two groups were performed using an unpaired two-tailed t-test. A *P*-value < 0.05 was considered statistically significant. Statistical analyses and graphing were performed using GraphPad Prism 9.0 software.

Results

SAB improves cardiac function in rats with myocardial infarction

To evaluate the effects of Salvianolic Acid B (SAB) on cardiac function following myocardial infarction (MI), we assessed left ventricular function via echocardiography 28 days post-surgery. As shown in **Figure 1A**, compared with the Sham group (72.4 ± 2.1%), the left ventricular ejection fraction (LVEF) in the MI group was significantly reduced (31.8 ± 2.3%, P < 0.01). SAB treatment significantly improved LVEF (54.2 ± 2.6%, P < 0.01 vs. MI), and a similar improvement was observed in the β3-AR agonist group (58.7 ± 2.4%, P < 0.01 vs. MI) with no significant difference between the SAB group and the agonist group (P > 0.05) left ventricular fractional shortening (LVFS) showed a similar trend (**Figure 1B**). LVFS in the MI group (15.2 ± 1.8%) was significantly lower than that in the Sham group (35.6 ± 1.9%) (P < 0.01). Both SAB treatment (24.8 ± 2.1%, P < 0.01 vs. MI) and β3-AR agonist treatment (26.3 ± 2.0%, P < 0.01 vs. MI) significant-

ly improved LVFS. Measurements of left ventricular end-diastolic diameter (LVEDD) and end-systolic diameter (LVESD) (**Figure 1C**, **1D**) showed that in the MI group, LVEDD (8.9 ± 0.3 mm) and LVESD (7.5 ± 0.3 mm) were significantly increased compared to the Sham group (6.1 ± 0.2 mm and 3.9 ± 0.2 mm) (both $P < 0.01$). SAB treatment significantly reduced LVEDD (7.2 ± 0.3 mm, $P < 0.01$ vs. MI) and LVESD (5.4 ± 0.3 mm, $P < 0.01$ vs. MI); similar results were observed in the β3-AR agonist group (LVEDD: 7.0 ± 0.2 mm, LVESD: 5.2 ± 0.2 mm, both $P < 0.01$ vs. MI).

SAB alleviates myocardial pathological damage in rats with myocardial infarction

The effects of SAB on post-myocardial infarction pathological changes were assessed via histological staining. Masson's trichrome staining revealed (**Figure 2A**) that the area of myocardial fibrosis was significantly increased in the MI group (22.4 ± 1.8%), whereas only minimal fibrosis was observed in the Sham group (1.2 ± 0.3%, $P < 0.01$). SAB treatment significantly reduced the area of fibrosis (8.9 ± 1.2%, $P < 0.01$ vs. MI), and a similar reduction was observed in the β3-AR agonist group (7.6 ± 1.1%, $P < 0.01$ vs. MI). TTC staining was used to assess the infarct size (**Figure 2B**). The infarct size in the MI group was 28.5 ± 2.2%, whereas no infarct was observed in the Sham group ($P < 0.01$). SAB treatment significantly reduced the infarct area (12.3 ± 1.5%, $P < 0.01$ vs. MI), and the β3-AR agonist group also showed a significant reduction in infarct area (10.8 ± 1.4%, $P < 0.01$ vs. MI). H&E staining was used to assess the area of myocardial necrosis (**Figure 2C**). The area of necrosis in the MI group reached 32.1 ± 2.4%, while only minimal necrosis was observed in the Sham group (0.5 ± 0.2%, $P < 0.01$). SAB treatment significantly reduced the area of necrosis (14.6 ± 1.8%, $P < 0.01$ vs. MI), and the area of necrosis was also significantly reduced in the β3-AR agonist group (12.9 ± 1.6%, $P < 0.01$ vs. MI).

SAB promotes myocardial cell proliferation in rats with myocardial infarction

Myocardial cell proliferation was assessed using Ki67 immunohistochemical staining (**Figure 3**). The percentage of Ki67-positive cells in the myocardial tissue of the Sham group was extremely low (0.8 ± 0.2%). The Ki67-positive cell rate in the MI group (2.3 ± 0.3%) was significantly higher than that in the Sham group ($P < 0.01$). SAB treatment significantly increased the Ki67-positive cell rate (8.7 ± 0.8%, $P < 0.01$ vs. MI). A significant increase in the Ki67-positive cell rate was also observed in the β3-AR agonist group (9.2 ± 0.9%, $P < 0.01$ vs. MI), with no significant difference between the SAB group and the agonist group ($P > 0.05$).

Regulation of β3-AR and miR-1 expression by SAB in rats with myocardial infarction

To further explore the molecular mechanisms underlying the cardioprotective effects of SAB, we examined the expression levels of β3-AR and miR-1 in myocardial tissue. Western blot results showed (**Figure 4A**) that β3-AR protein was expressed at low levels in the MI group. SAB treatment significantly upregulated β3-AR expression (2.35 ± 0.18-fold, $P < 0.01$ vs. MI), and an upregulation of β3-AR expression was also observed in the β3-AR agonist group (2.52 ± 0.20-fold, $P < 0.01$ vs. MI). When administered in combination with a β3-AR antagonist, the SAB-induced upregulation of β3-AR was significantly blocked (1.18 ± 0.10-fold, $P < 0.01$ vs. MI + SAB). qPCR analysis of miR-1 expression levels showed (**Figure 4B**) that miR-1 was highly expressed in the MI group. SAB treatment significantly downregulated miR-1 expression (0.42 ± 0.05-fold, $P < 0.01$ vs. MI), and the β3-AR agonist also significantly downregulated miR-1 expression (0.38 ± 0.04-fold, $P < 0.01$ vs. MI). Following co-administration of a β3-AR antagonist, the SAB-induced downregulation of miR-1 was significantly blocked (0.89 ± 0.08-fold, $P < 0.01$ vs. MI + SAB). Furthermore, miR-1 expression was significantly elevated in the miR-1 mimic group (3.85 ± 0.25-fold, $P < 0.01$ vs. MI + SAB), confirming the validity of the overexpression system.

The β3-AR/miR-1 axis mediates the cardioprotective effects of SAB

To verify whether miR-1 is a key downstream effector molecule responsible for the protective effects of SAB, we conducted a rescue experiment using a miR-1 mimetic. Cardiac function tests revealed (**Figure 5A**, **5B**) that SAB treatment significantly improved LVEF and LVFS, whereas the beneficial effects of SAB were significantly attenuated following co-administration of the miR-1 mimetic (LVEF: decreased

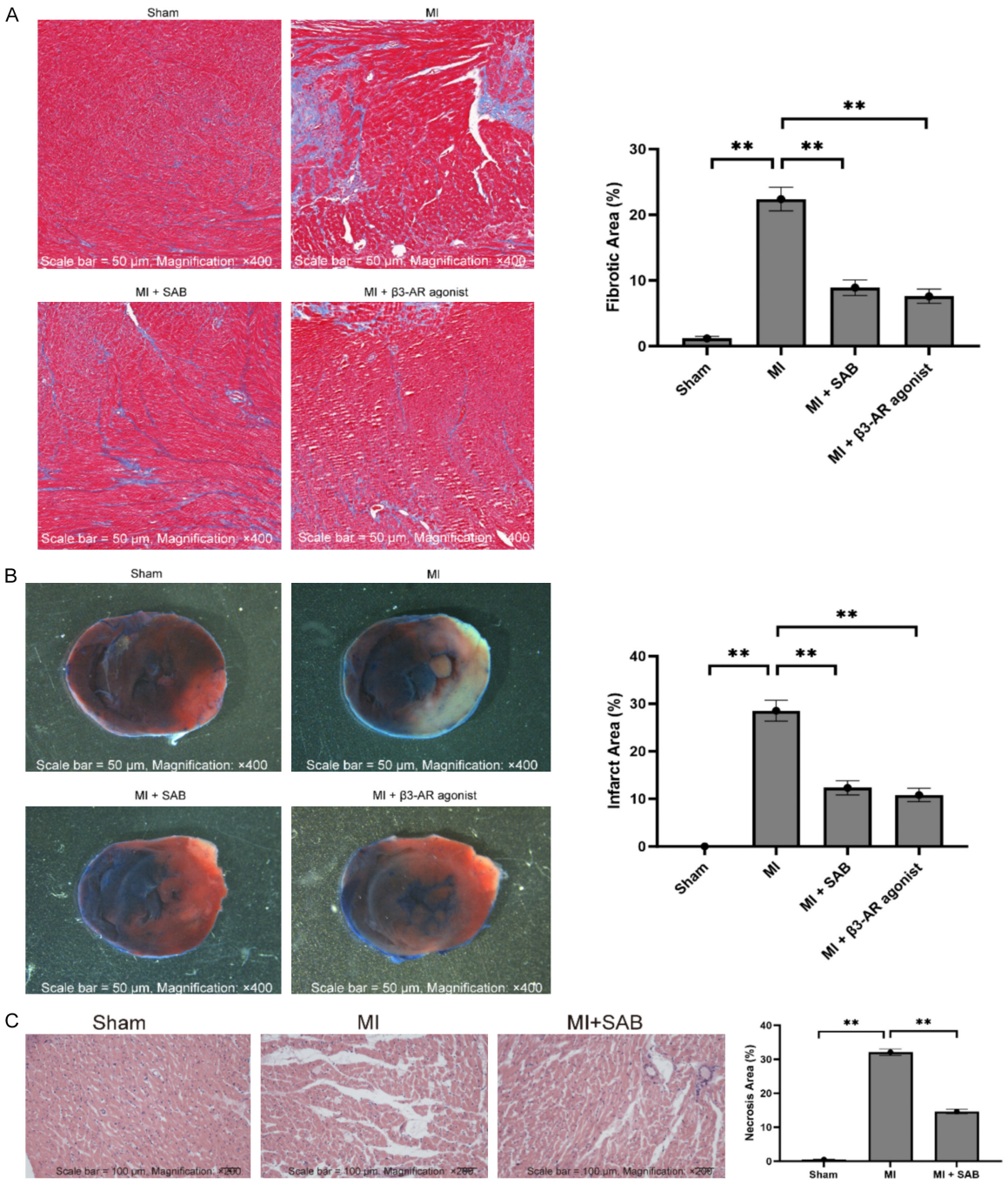

Figure 2. SAB reduces infarct size, fibrosis, and necrosis in MI rats. A: Representative Masson's trichrome-stained sections (collagen in blue) and quantitative analysis of fibrotic area (%). Scale bar = 50 μm, Magnification: ×400. B: Representative TTC-stained heart slices (viable tissue in red, infarct in pale) and quantitative analysis of infarct area (%). Scale bar = 50 μm, Magnification: ×400. C: Representative H&E-stained sections and quantitative analysis of necrosis area (%). Scale bar = 100 μm, Magnification: ×200. Data are presented as mean ± SEM (n = 6-8 per group). $^{**}P < 0.01$ vs. MI group (one-way ANOVA with Tukey's post hoc test).

from 54.2 ± 2.6% to 35.1 ± 2.5%, P < 0.01 vs. MI + SAB; LVFS: decreased from 24.8 ± 2.1% to 18.1 ± 1.9%, P < 0.01 vs. MI + SAB). Pathological injury assessment results showed (**Figure 5C**, **5D**), SAB treatment significantly reduced infarct area and fibrosis area, whereas the miR-1 mimic significantly reversed the protective effects of SAB (infarct area: increased from 12.3 ± 1.5% to 24.1 ± 2.0%, P < 0.01 vs. MI + SAB; fibrosis area: increased from 8.9 ± 1.2% to

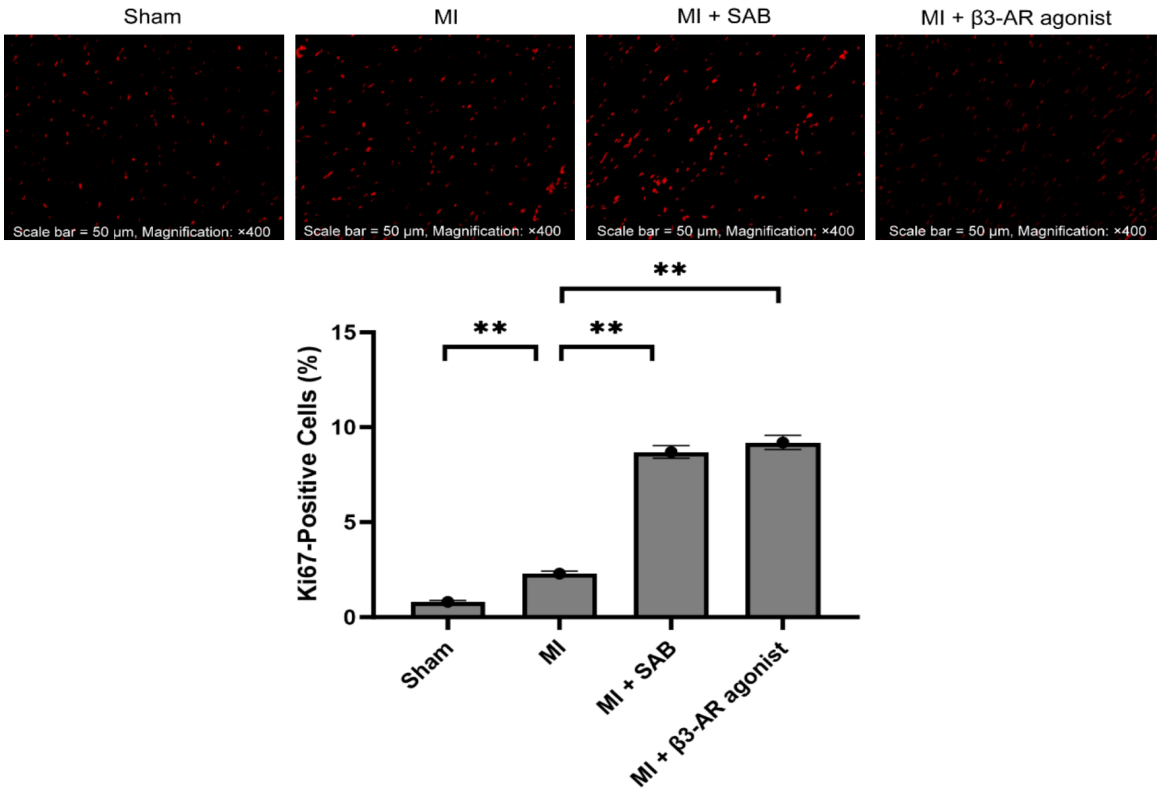

Figure 3. SAB promotes cardiomyocyte proliferation in MI rats Representative immunohistochemical images of Ki67 (brown nuclei) in heart sections from the indicated groups. Scale bar = 50 μm, Magnification: ×400. Quantitative analysis of Ki67-positive cardiomyocytes (%) in the peri-infarct region. Data are presented as mean ± SEM (n = 6-8 per group). $^{**}P < 0.01$ vs. MI group (one-way ANOVA with Tukey's post hoc test).

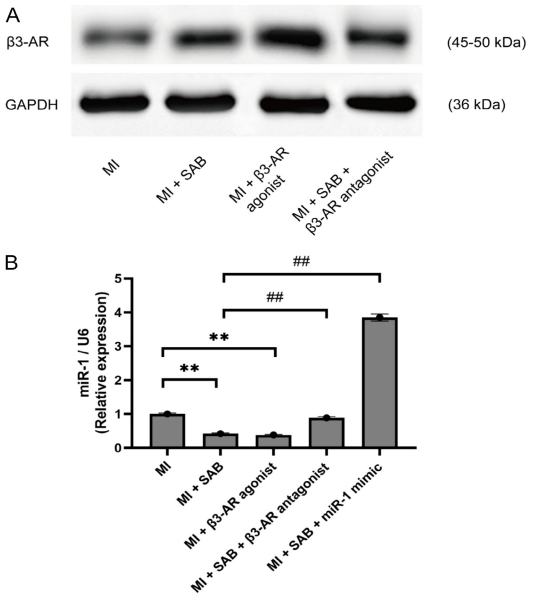

Figure 4. SAB regulates β3-AR and miR-1 expression in MI rats. A: Protein expression of β3-AR determined by Western blot. Representative blots are shown, and densitometric quantification is normalized to GAPDH. B: miR-1 expression determined by qPCR, normalized to U6 snRNA. Data are presented as mean ± SEM (n = 6-8 per group). $^{**}P < 0.01$ vs. MI group; $^{\#\#}P < 0.01$ vs. MI + SAB group (one-way ANOVA with Tukey's post hoc test).

19.3 ± 1.6%, P < 0.01 vs. MI + SAB). Cell proliferation assays revealed (**Figure 5E**) that SAB treatment significantly increased the Ki67-positive cell rate (8.7 ± 0.8%), while the miR-1 mimic completely abolished the proliferative effect of SAB (3.1 ± 0.4%, P < 0.01 vs. MI + SAB), restoring it to levels close to those of the MI group.

SAB upregulates CDK4 and cyclin D1 expression by downregulating miR-1

To elucidate the downstream molecular events following SAB-induced downregulation of miR-1, we examined the protein expression levels of the miR-1 target genes CDK4 and Cyclin D1. Western blot results showed (**Figure 6A**) that CDK4 and Cyclin D1 were expressed at low levels in the MI group. SAB treatment significantly

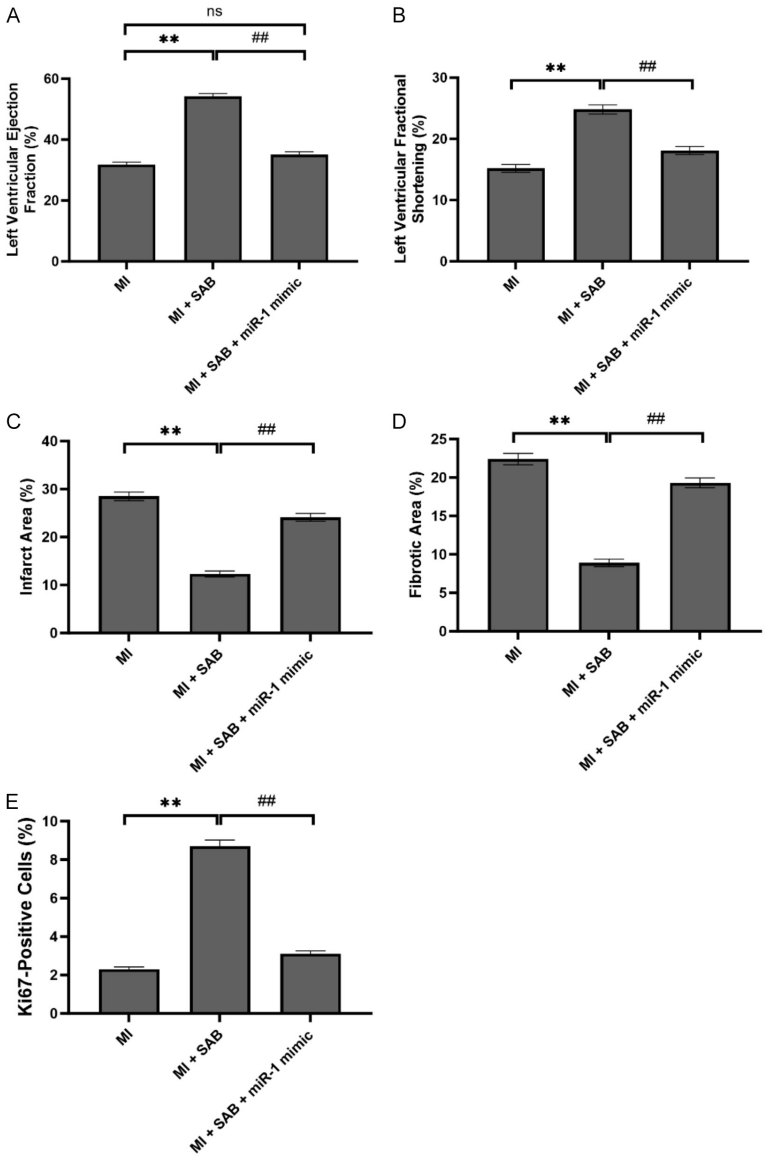

Figure 5. The β3-AR/miR-1 axis is essential for SAB-induced cardioprotection and cardiomyocyte proliferation in MI rats. (A) Left ventricular ejection fraction (LVEF, %) and (B) left ventricular fractional shortening (LVFS, %) measured by echocardiography at 28 days after MI. (C) Infarct area (%) determined by TTC staining. (D) Fibrotic area (%) assessed by Masson's trichrome staining. (E) Quantification of Ki67-positive cardiomyocytes (%) in the peri-infarct region by immunohistochemistry. All panels show data from three key groups: MI, MI + SAB, and MI + SAB + miR-1 mimic. Data are presented as mean ± SEM (n = 6-8 per group). $^{**}P < 0.01$ vs. MI group; $^{\#\#}P < 0.01$ vs. MI + SAB group (one-way ANOVA with Tukey's post hoc test).

upregulated the expression of CDK4 (2.48 ± 0.18-fold, P < 0.01 vs. MI) and Cyclin D1 (2.62 ± 0.20-fold, P < 0.01 vs. MI). Upon co-administration of the miR-1 mimetic, the SAB-induced upregulation of CDK4 (1.22 ± 0.10-fold, P < 0.01 vs. MI + SAB) and Cyclin D1 (1.18 ± 0.09-fold, P < 0.01 vs. MI + SAB) were significantly blocked (**Figure 6B**). Conversely, co-administration of a miR-1 inhibitor further enhanced the SAB-induced upregulation of CDK4 (3.65 ± 0.25-fold, P < 0.01 vs. MI + SAB) and Cyclin D1 (3.92 ± 0.28-fold, P < 0.01 vs. MI + SAB) (**Figure 6C**).

In vitro validation of the β3-AR/miR-1 axis in cardiomyocytes

To further validate the regulatory axis identified in vivo, we conducted in vitro experiments using a hypoxia/reoxygenation (H/R) model in primary cardiomyocytes. EdU incorporation results showed (**Figure 7A**) that the EdU-positive cell percentage in the H/R group was 4.2 ± 0.5%. SAB treatment significantly increased the EdU-positive cell percentage (18.6 ± 1.4%, P < 0.01 vs. H/R), whereas the proliferative effect of SAB was completely blocked upon co-administration of a β3-AR antagonist (6.8 ± 0.7%, P < 0.01 vs. H/R + SAB).

qPCR results showed (**Figure 7B**) that SAB treatment significantly downregulated miR-1 expression (0.38 ± 0.04-fold, P < 0.01 vs. H/R) and simultaneously significantly upregulated Cyclin D1 expression (2.85 ± 0.22-fold, P < 0.01 vs. H/R). Results from the dual-luciferase reporter assay (**Figure 7C**) showed that the miR-1 mimic significantly reduced the luciferase activity of the CDK4 3'UTR reporter (0.42 ± 0.05-fold, P < 0.01 vs. NC), whereas the miR-1 inhibitor significantly enhanced its activity (1.85 ± 0.12-fold, P < 0.01 vs. NC), confirming that miR-1 directly targets the 3'UTR region of CDK4.

Discussion

This study is the first to demonstrate that Salvianolic Acid B (SAB) promotes cardiomyo-

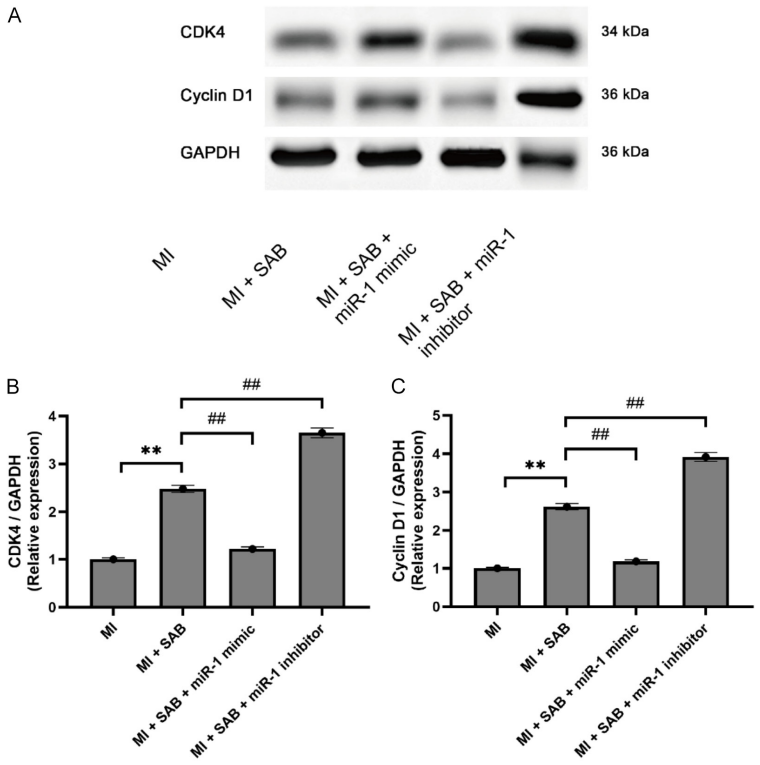

Figure 6. SAB upregulates CDK4 and Cyclin D1 via miR-1 downregulation. A: Representative Western blot images of CDK4, Cyclin D1, and GAPDH (loading control) in heart tissues from the indicated groups. B, C: Quantitative densitometric analysis of CDK4 (B) and Cyclin D1 (C) normalized to GAPDH. Data are presented as mean ± SEM (n = 6-8 per group). $^{**}P < 0.01$ vs. MI group; $^{\#\#}P < 0.01$ vs. MI + SAB group (one-way ANOVA with Tukey's post hoc test).

cyte proliferation by activating the β3-adrenergic receptor (β3-AR)/miRNA-1 (miR-1) signaling axis, thereby improving cardiac function and reducing pathological remodeling following myocardial infarction (MI). This finding not only expands the cardioprotective effects of SAB from the traditional concept of "cell protection" to a new dimension of "cell regeneration", but also provides a novel perspective on the role of β3-AR in myocardial repair, while establishing the pivotal role of the "GPCR → miRNA → cell cycle" regulatory pathway in myocardial regeneration.

As the primary water-soluble active component of Salvia miltiorrhiza, SAB has been previously demonstrated to possess multiple cardioprotective effects, including anti-inflammatory, antioxidant, anti-apoptotic, and microcirculation-improving properties [28, 29]. However, whether SAB can directly stimulate terminally differentiated adult cardiomyocytes to re-enter the cell cycle and proliferate has not been previously reported. This study consistently demonstrated through in vivo and in vitro experiments that SAB treatment significantly increased the proportion of Ki67-positive cardiomyocytes in the peri-infarct zone and elevated the EdU-positive cell rate in an in vitro hypoxia/reoxygenation (H/R) model, providing direct evidence of SAB's direct proliferative effects. This finding elevates the role of SAB from "limiting damage" to the higher dimension of "active repair", providing a new candidate drug for cardiac regeneration following myocardial infarction [30]. This regenerative effect distinguishes SAB from other cardioprotective agents such as propofol, which has been reported to protect against myocardial ischemia-reperfusion injury primarily through anti-apoptotic mechanisms involving the ERK MAPK/NF-KB signaling axis [31]. While inhibiting apoptosis is undoubtedly beneficial for limiting infarct size, promoting active cardiomyocyte proliferation may offer additional advantages for long-term functional recovery by replacing lost myocardial tissue.

β3-AR is an "atypical" member of the adrenergic receptor family. Previous studies have primarily focused on its role in mediating metabolic functions such as lipolysis and thermogenesis, as well as its anti-apoptotic effects in myocardial ischemia/reperfusion injury and heart failure through activation of the eNOS pathway [32]. However, there have been no previous reports on whether β3-AR participates in the regulation of cardiomyocyte proliferation. This study found that SAB treatment significantly upregulated β3-AR expression in cardiac tissue, and the selective β3-AR agonist BRL37344 was able to mimic the proliferative effects of SAB, whereas the β3-AR antagonist SR59230A completely blocked the effects of SAB. These results establish, for the first time, a direct link

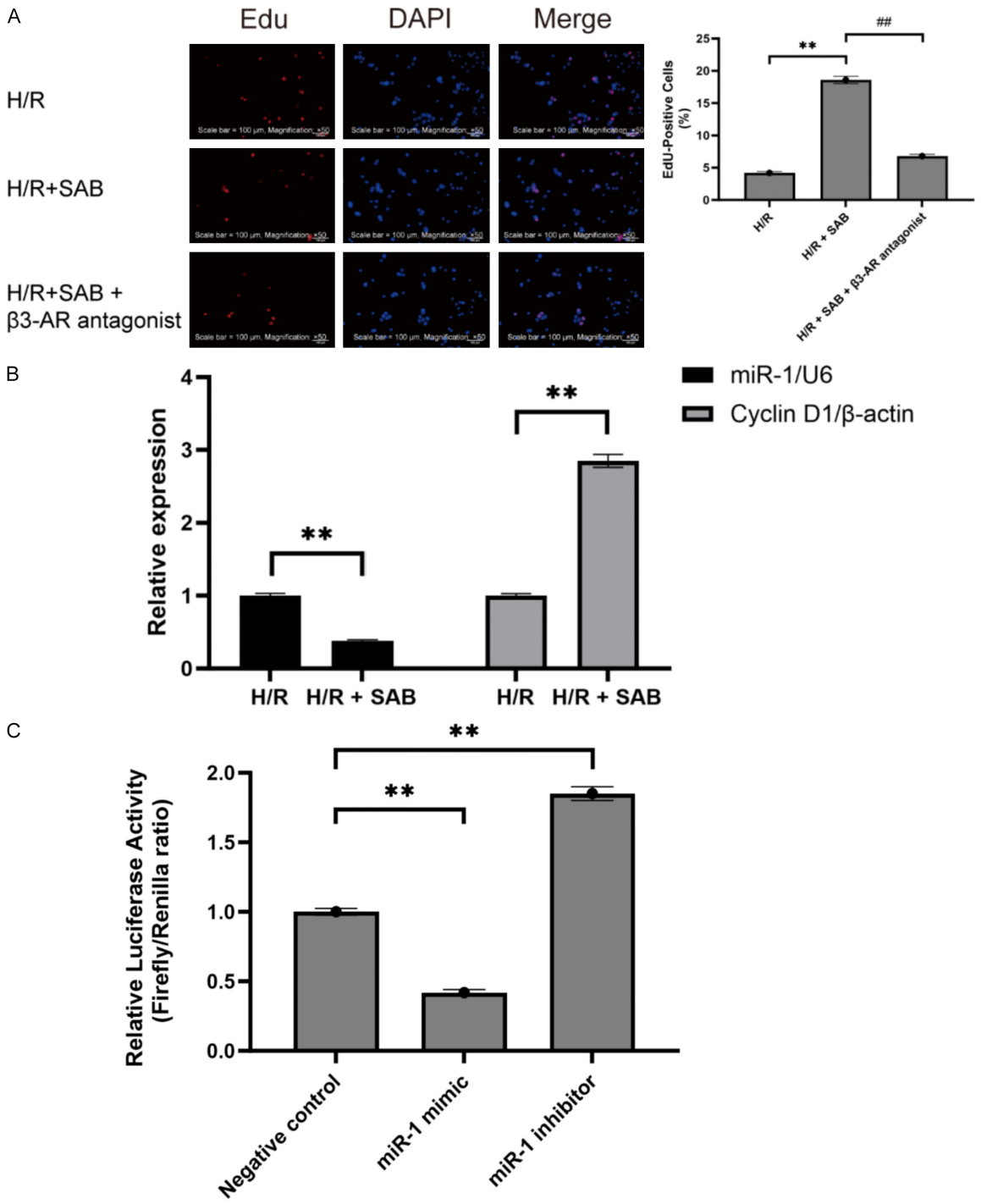

Figure 7. In vitro validation of the β3-AR/miR-1 axis in cardiomyocytes. A: Representative EdU staining images (red, proliferating cells; blue, DAPI-stained nuclei) and quantification of EdU-positive cells in H/R-treated neonatal rat cardiomyocytes. Scale bar = 100 μm, Magnification: ×50. B: Relative expression of miR-1 and Cyclin D1 determined by qPCR. C: Dual-luciferase reporter assay showing miR-1 directly targets the 3'UTR of CDK4. Data are presented as mean ± SEM from three independent experiments. $^{**}P < 0.01$ vs. H/R group (panels A, B); $^{**}P < 0.01$ vs. NC group (panel C); $^{\#\#}P < 0.01$ vs. H/R + SAB group (one-way ANOVA with Tukey's post hoc test).

between β3-AR and cardiac cell cycle regulation, revealing a novel function of β3-AR in cardiac repair. Unlike previous studies that primarily focused on the anti-apoptotic effects of β3-

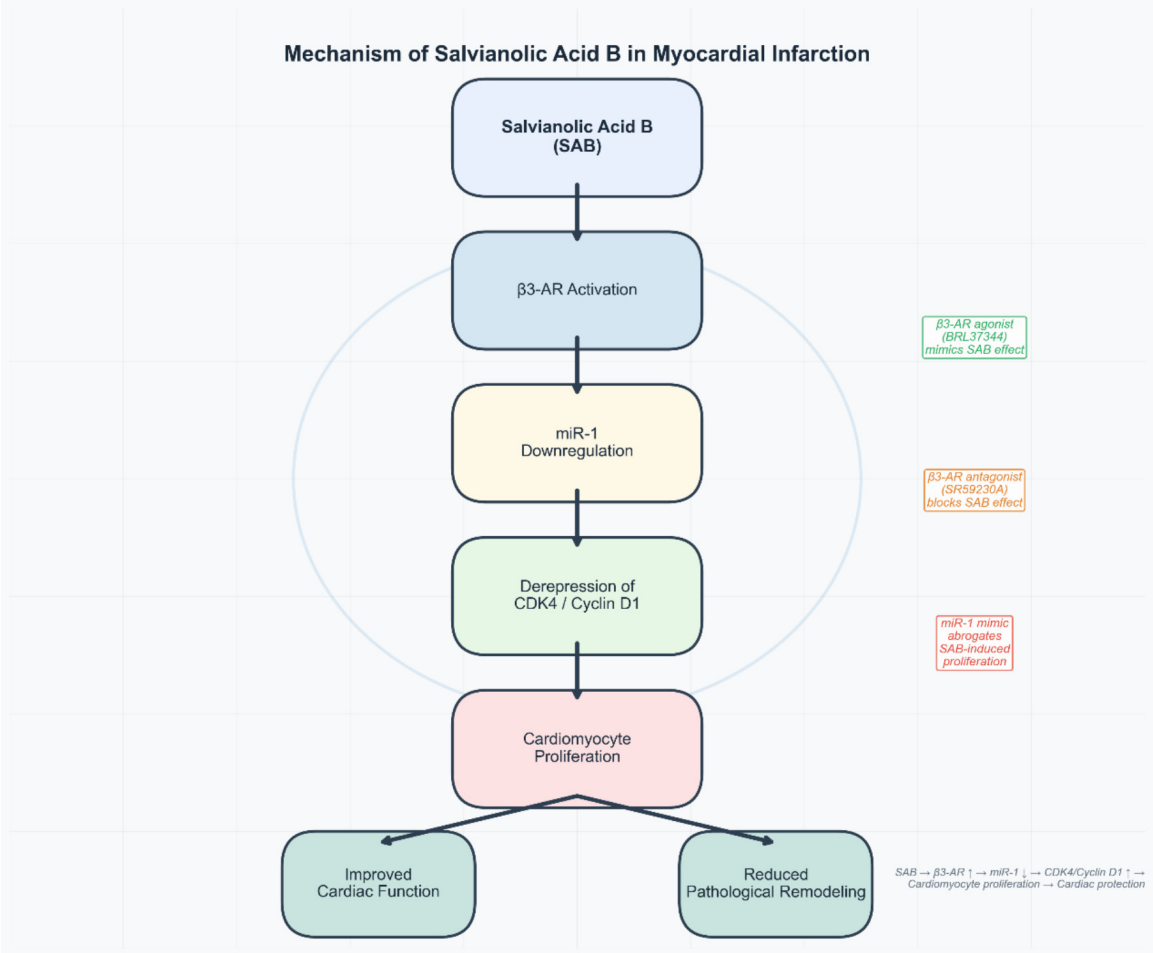

Figure 8. Schematic illustration of the proposed mechanism. Salvianolic acid B (SAB) activates β3-adrenergic receptor (β3-AR), leading to downregulation of miR-1. This relieves the miR-1-mediated repression of CDK4 and Cyclin D1, thereby promoting cardiomyocyte proliferation and ultimately improving cardiac function while reducing pathological remodeling. Pharmacological interventions (β3-AR agonist, antagonist, and miR-1 mimic) used to validate the axis are indicated.

AR [33], this study demonstrates that β3-AR activation can also drive cardiac cell proliferation, a finding that expands the application prospects of β3-AR as a cardiac protective target.

miR-1 is one of the most abundantly expressed miRNAs in the heart and is widely recognized as a key "braking" molecule that maintains the terminal differentiation state of cardiomyocytes [34]. This study confirmed that miR-1 expression was significantly elevated in the myocardial tissue of MI rats, whereas SAB treatment significantly downregulated miR-1 expression, and this effect could be blocked by a β3-AR antagonist. More importantly, rescue experiments using miR-1 mimics demonstrated that miR-1 overexpression completely abolished the beneficial effects of SAB on cardiac function, pathological damage, and cardiomyocyte proliferation, whereas miR-1 inhibitors further enhanced SAB-induced upregulation of CDK4 and Cyclin D1. These results strongly demonstrate that miR-1 is a key downstream effector molecule through which SAB exerts its proliferative effects via β3-AR. This finding introduces the "GPCR → miRNA" regulatory axis into the field of cardiac muscle regeneration, providing a new paradigm for understanding how natural compounds finely regulate gene expression networks [35].

miR-1 exerts its "braking" effect by specifically inhibiting multiple positive regulators of the cell cycle, among which CDK4 and Cyclin D1 are central molecules that initiate the G1/S phase transition of the cell cycle [18, 19]. This study confirmed via Western blot that SAB

treatment significantly upregulates the protein expression of CDK4 and Cyclin D1, and that this effect can be blocked by miR-1 mimics and further enhanced by miR-1 inhibitors. Furthermore, a dual-luciferase reporter assay directly confirmed that miR-1 specifically binds to the 3'UTR region of CDK4, providing direct molecular evidence for miR-1's regulation of CDK4. These results comprehensively elucidate the molecular cascade of the SAB → β3-AR → miR-1 → CDK4/Cyclin D1 signaling axis.

In recent years, significant progress has been made in research on promoting cardiac muscle regeneration. Previous studies have shown that certain natural compounds, such as resveratrol and ginsenosides, can promote cardiomyocyte proliferation by regulating specific miRNAs [20]; however, the upstream receptor mechanisms remain unclear. This study is the first to directly link the action of SAB to β3-AR and reveals the complete pathway through which it regulates downstream cyclins via miR-1. Unlike the anti-apoptotic effects of β3-AR reported by Mohammed et al. [16], this study found that β3-AR activation can also drive cell cycle re-entry, adding new insights into the multifaceted protective functions of β3-AR in the heart. Furthermore, consistent with the findings of Mu et al. regarding the role of the miR-1 family in regulating fibrosis following myocardial infarction [18], this study further positions miR-1 downstream of β3-AR, establishing a complete signaling pathway from cell membrane receptors to nuclear cell cycle regulation.

Based on the findings of this study, we propose a dual-target therapeutic strategy combining β3-AR activation with miR-1 inhibition. On the one hand, SAB or β3-AR agonists can promote proliferation by activating the receptor; on the other hand, miR-1 inhibitors (such as antagomirs) can further amplify this effect. This multi-tiered intervention strategy may be more effective than single-target approaches in overcoming the inherent barriers to regenerative capacity in adult cardiomyocytes [19]. Although the translation from basic research to clinical practice still faces numerous challenges, such as drug delivery efficiency, targeting specificity, and potential arrhythmia risks, the findings of this study provide a new theoretical foundation for the development of combination therapies to promote myocardial regeneration.

This study has the following limitations: First, in vivo proliferation experiments primarily utilized Ki67 immunohistochemistry; although this is a classic marker of proliferation, combining it with multiple indicators such as pH3 and Aurora B would provide more comprehensive evidence. Second, in vitro experiments primarily used neonatal rat cardiomyocytes, which have higher proliferative capacity than adult cardiomyocytes; further validation should be conducted in adult cardiomyocytes or cardiomyocytes derived from human induced pluripotent stem cells. Third, the optimal dosage, timing, and duration of SAB administration still require systematic optimization; fourth, the precise molecular mechanisms by which β3-AR regulates miR-1 expression (such as transcription factors, epigenetic modifications, or RNA processing) require further investigation; fifth, this study did not validate the necessity of β3-AR in gene-knockout animal models; future studies could utilize β3-AR knockout mice to further confirm this.

Conclusion

In summary, this study has, for the first time, revealed a novel mechanism by which SAB promotes cardiomyocyte proliferation, improves cardiac function following myocardial infarction, and alleviates pathological remodeling by activating the β3-AR/miR-1 axis, thereby lifting the inhibitory effect of miR-1 on CDK4 and Cyclin D1 (**Figure 8**). This finding not only provides a novel mechanistic explanation for the cardioprotective effects of SAB but also establishes the β3-AR/miR-1 axis as a potential therapeutic target for cardiac repair following myocardial infarction. Based on the dual-target strategy of "activating protective receptors + lifting proliferation inhibition", this study provides important theoretical and experimental foundations for the development of novel therapies to promote myocardial regeneration.

Acknowledgements

This study was supported by Guangzhou Science and Technology plan project (20220102-0020); Guangzhou School (College) and Enterprise Joint Funding Project (2025A03J3592); 2024A03J0654 Guangzhou School (College) and Enterprise Joint Funding Project (2024-A03J0654).

Disclosure of conflict of interest

None.

Address correspondence to: Qiang Zhao, Department of Cardiology, Guangzhou Red Cross Hospital of Jinan University, No. 396 Tongfuzhong Road, Haizhu District, Guangzhou 510220, Guangdong, China. Tel: +86-020-61886188; E-mail: zhaoqiang1020430@126.com

References

[1] Chen Q, Xu Q, Zhu H, Wang J, Sun N, Bian H, Li Y and Lin C. Salvianolic acid B promotes angiogenesis and inhibits cardiomyocyte apoptosis by regulating autophagy in myocardial ischemia. Chin Med 2023; 18: 155.

[2] Mu L, Dong R, Li C, Chen J, Huang Y, Li T and Guo B. ROS responsive conductive microspheres loaded with salvianolic acid B as adipose derived stem cell carriers for acute myocardial infarction treatment. Biomaterials 2025; 314: 122849.

[3] Zhou R, Gao J, Xiang C, Liu Z, Zhang Y, Zhang J and Yang H. Salvianolic acid A attenuated myocardial infarction-induced apoptosis and inflammation by activating Trx. Naunyn Schmiedebergs Arch Pharmacol 2020; 393: 991-1002.

[4] Shen Y, Shen X, Wang S, Zhang Y, Wang Y, Ding Y, Shen J, Zhao J, Qin H, Xu Y, Zhou Q, Wang X and Shen J. Protective effects of salvianolic acid B on rat ferroptosis in myocardial infarction through upregulating the Nrf2 signaling pathway. Int Immunopharmacol 2022; 112: 109257.

[5] Yang LL, Cao C, Kang J, Liu ZX, Meng HX, Liu JX and Li L. Protection of vasodilatory function in rats with post-infarction heart failure by salvianolic acid B via modulating Piezo1 channel. Zhongguo Zhong Yao Za Zhi 2024; 49: 5566-5576.

[6] Liu H, Liu W, Qiu H, Zou D, Cai H, Chen Q, Zheng C and Xu D. Salvianolic acid B protects against myocardial ischaemia-reperfusion injury in rats via inhibiting high mobility group box 1 protein expression through the PI3K/Akt signalling pathway. Naunyn Schmiedebergs Arch Pharmacol 2020; 393: 1527-1539.

[7] Yang Y, Yang J, Fu W, Zhou P, He Y, Fang M, Wan H and Zhou H. Pharmacokinetic comparison of nine bioactive compounds of Guanxinshutong Capsule in normal and acute myocardial infarction rats. Eur J Drug Metab Pharmacokinet 2022; 47: 653-665.

[8] Bi SJ, Dong XY, Wang ZY, Fu SJ, Li CL, Wang ZY, Xie F, Chen XY, Xu H, Cai XJ and Zhang MX. Salvianolic acid B alleviates neurological injury by upregulating stanniocalcin 1 expression. Ann Transl Med 2022; 10: 739.

[9] Yan J, Liu H, Shang J, Fang Q, Ye J, Lu X and Fan X. Protective effects of Shexiang-Tongxin dropping pill against acute myocardial infarction in rats through inhibition of apoptosis and ERK/MAPK signaling pathways. Heliyon 2024; 10: e39939.

[10] Zhang CJ, Qu XY, Yu ZY, Yang J, Zhu B, Zhong LY, Sun J, He JH, Zhu YX, Dong L and Xu WJ. Research of the dynamic regulatory mechanism of Compound Danshen Dripping Pills on myocardial infarction based on metabolic trajectory analysis. Phytomedicine 2024; 130: 155626.

[11] An J, Du Y, Li X, Bao Q, Guo Y, Song Y and Jia Y. Myocardial protective effect of sacubitril-valsartan on rats with acute myocardial infarction. Perfusion 2022; 37: 208-215.

[12] Qiao P, Wang Y, Zhu K, Zheng D, Song Y, Jiang D, Qin C and Lan X. Noninvasive monitoring of reparative fibrosis after myocardial infarction in rats using ^{68}Ga-FAPI-04 PET/CT. Mol Pharm 2022; 19: 4171-4178.

[13] Li F, Zhu H, Chang Z and Li Y. Gentiopicroside alleviates acute myocardial infarction injury in rats by disrupting Nrf2/NLRP3 signaling. Exp Biol Med (Maywood) 2023; 248: 1254-1266.

[14] Han BJ, Cao GY, Jia LY, Zheng G, Zhang L, Sheng P, Xie JZ and Zhang CF. Cardioprotective effects of tetrahydropalmatine on acute myocardial infarction in rats. Am J Chin Med 2022; 50: 1887-1904.

[15] Jinawong K, Piamsiri C, Apaijai N, Maneechote C, Arunsak B, Nawara W, Thonusin C, Pintana H, Chattipakorn N and Chattipakorn SC. Modulating mitochondrial dynamics mitigates cognitive impairment in rats with myocardial infarction. Curr Neuropharmacol 2024; 22: 1749-1760.

[16] Mohammed EN, Soliman AM and Mohamed AS. Modulatory effect of Ovothiol-A on myocardial infarction induced by epinephrine in rats. J Food Biochem 2022; 46: e14296.

[17] Xia R, Zhu T, Zhang Y, He B, Chen Y, Wang L, Zhou Y, Liao J, Zheng J, Li Y, Lv F and Gao F. Myocardial infarction size as an independent predictor of intramyocardial haemorrhage in acute reperfused myocardial ischaemic rats. Eur J Med Res 2022; 27: 220.

[18] Nair RS, Sobhan PK, Shenoy SJ, Prabhu MA, Kumar V, Ramachandran S and Anilkumar TV. Mitigation of fibrosis after myocardial infarction in rats by using a porcine cholecyst extracellular matrix. Comp Med 2023; 73: 312-323.

[19] Beyazcicek E and Beyazcicek O. Protective effects of lacticaseibacillus rhamnosus on isoprenaline-induced myocardial infarction in rats. J Appl Microbiol 2023; 134: lxac008.

[20] Feliciano RDS, Atum ALB, Ruiz ÉGDS, Serra AJ, Antônio EL, Manchini MT, Silva JMA, Tucci PJF, Nathanson L, Morris M, Chavantes MC and Silva Júnior JA. Photobiomodulation therapy on myocardial infarction in rats: transcriptional and posttranscriptional implications to cardiac remodeling. Lasers Surg Med 2021; 53: 1247-1257.

[21] Jinawong K, Piamsiri C, Apaijai N, Maneechote C, Pintana H, Chunchai T, Arunsak B, Chattipakorn N and Chattipakorn SC. Treatment with apoptosis inhibitor restores cognitive impairment in rats with myocardial infarction. Biochim Biophys Acta Mol Basis Dis 2023; 1869: 166809.

[22] Ramakrishna K and Krishnamurthy S. Indole-3-carbinol ameliorated the isoproterenol-induced myocardial infarction via multimodal mechanisms in Wistar rats. Nat Prod Res 2022; 36: 6044-6049.

[23] Lin X, Liu W, Chu Y, Zhang H, Zeng L, Lin Y, Kang K, Peng F, Lin J, Huang C and Chai D. Activation of AHR by ITE improves cardiac remodelling and function in rats after myocardial infarction. ESC Heart Fail 2023; 10: 3622-3636.

[24] Gao X, Ni C, Song Y, Xie X, Zhang S, Chen Y, Wu H, Shi H, Zhang B, Huang F, Wang C and Wu X. Dan-shen Yin attenuates myocardial fibrosis after myocardial infarction in rats: molecular mechanism insights by integrated transcriptomics and network pharmacology analysis and experimental validation. J Ethnopharmacol 2025; 338: 119070.

[25] Mo C, Han H, Tang X, Lu X, Wei Y, Luo D and Zhou Z. Protein kinase TBK1/IKKε inhibitor amlexanox improves cardiac function after acute myocardial infarction in rats. Panminerva Med 2023; 65: 343-350.

[26] Wu Z, Yu L, Li X and Li X. Protective mechanism of trimetazidine in myocardial cells in myocardial infarction rats through ERK signaling pathway. Biomed Res Int 2021; 2021: 9924549.

[27] Jia J, Zhao XA, Tao SM, Wang JW, Zhang RL, Dai HL, Zhang XJ, Han MH, Yang B, Li Y and Li JT. Icariin improves cardiac function and remodeling via the TGF-β1/Smad signaling pathway in rats following myocardial infarction. Eur J Med Res 2023; 28: 607.

[28] Cheng XJ, Li L and Xin BQ. MiR-124 regulates the inflammation and apoptosis in myocardial infarction rats by targeting STAT3. Cardiovasc Toxicol 2021; 21: 710-720.

[29] Souza LM, Okoshi MP, Gomes MJ, Gatto M, Rodrigues EA, Pontes THD, Damatto FC, Oliveira LRS, Borim PA, Lima ARR, Zornoff LAM, Okoshi K and Pagan LU. Effects of late aerobic exercise on cardiac remodeling of rats with small-sized myocardial infarction. Arq Bras Cardiol 2021; 116: 784-792.

[30] Liu Y, Zhong C, Si J, Chen S, Kang L and Xu B. The impact of sacubitril/valsartan on cardiac fibrosis early after myocardial infarction in hypertensive rats. J Hypertens 2022; 40: 1822-1830.

[31] Li H, Tan J, Zou Z, Huang CG and Shi XY. Propofol post-conditioning protects against cardiomyocyte apoptosis in hypoxia/reoxygenation injury by suppressing nuclear factor-kappa B translocation via extracellular signal-regulated kinase mitogen-activated protein kinase pathway. Eur J Anaesthesiol 2011; 28: 525-534.

[32] Wang M, Wang M, Zhao J, Xu H, Xi Y and Yang H. Dengzhan Shengmai capsule attenuates cardiac fibrosis in post-myocardial infarction rats by regulating LTBP2 and TGF-β1/Smad3 pathway. Phytomedicine 2023; 116: 154849.

[33] Guo Q, Wu D, Jia D, Zhang X, Wu A, Lou L, Zhao M, Zhao M, Gao Y, Wang M, Liu M, Chen M and Zhang D. Bioinformatics prediction and experimental verification of a novel microRNA for myocardial fibrosis after myocardial infarction in rats. PeerJ 2023; 11: e14851.

[34] Zhang P, Fang Z, Zhao M, Yi B, Huang Y, Yang H, Guo N and Zhao C. Ethanol extract of Pueraria lobata improve acute myocardial infarction in rats via regulating gut microbiota and bile acid metabolism. Phytother Res 2023; 37: 5932-5946.

[35] Demir M, Altinoz E, Elbe H, Bicer Y, Yigitturk G, Karayakali M and Ballur AFH. Effects of pinealectomy and crocin treatment on rats with isoproterenol-induced myocardial infarction. Drug Chem Toxicol 2022; 45: 2576-2585.